

Exploiting Intelligent Reflecting Surfaces in Multi-Antenna Aided NOMA Systems

Xidong Mu, *Student Member, IEEE*, Yuanwei Liu, *Senior Member, IEEE*,
Li Guo, *Member, IEEE*, Jiaru Lin, *Member, IEEE*, and
Naofal Al-Dhahir, *Fellow, IEEE*

Abstract

This paper investigates a downlink multiple-input single-output intelligent reflecting surface (IRS) non-orthogonal multiple access (NOMA) system, where a base station (BS) serves multiple users with the aid of IRSs. Our goal is to maximize the sum rate of all users by jointly optimizing the active beamforming at the BS and the passive beamforming at the IRS, subject to successive interference cancellation decoding rate conditions and IRS reflecting elements constraints. In term of the characteristics of reflection amplitudes and phase shifts, we consider ideal and non-ideal IRS assumptions. To tackle the formulated non-convex problems, we propose efficient algorithms by invoking alternating optimization, which design the active beamforming and passive beamforming alternately. For the ideal IRS scenario, the two subproblems are solved by invoking the successive convex approximation technique. For the non-ideal IRS scenario, constant modulus IRS elements are further divided into continuous phase shifters and discrete phase shifters. To tackle the passive beamforming problem with continuous phase shifters, a novel algorithm is developed by utilizing the sequential rank-one constraint relaxation approach, which is guaranteed to find a locally optimal rank-one solution. Then, a quantization-based scheme is proposed for discrete phase shifters. Finally, numerical results illustrate that: i) the system sum rate can be significantly improved by deploying the IRS with our proposed algorithms; ii) 3-bit phase shifters are capable of achieving almost the same performance as the ideal IRS; iii) the proposed IRS-NOMA systems achieve higher system sum rate than the IRS-aided orthogonal multiple access system.

I. INTRODUCTION

Recently, intelligent reflecting surface (IRS) aided transmission has drawn significant attention due to its superior performance in enhancing spectrum and energy efficiency enhancement for

Part of this work has been submitted to the IEEE International Conference on Communications (ICC), Dublin, Ireland, June 7-11, 2020. [1]

X. Mu, L. Guo, and J. Lin are with Beijing University of Posts and Telecommunications, Beijing, China. (email:{muxidong, guoli, jrlin}@bupt.edu.cn).

Y. Liu is with Queen Mary University of London, London, UK. (email:yuanwei.liu@qmul.ac.uk).

N. Al-Dhahir is with the Department of Electrical and Computer Engineering, The University of Texas at Dallas, Richardson, TX 75080 USA.(e-mail: aldhahir@utdallas.edu).

wireless communication networks [2,3]. Equipped with a large number of low-cost passive reflecting elements, IRSs are able to change the signal propagation characteristics by smartly adjusting the phase shift of each element [3]. For example, if the transmitter and receiver are blocked by an obstacle, an IRS can be carefully deployed to create an extra path to enhance the received signal strength. Compared with existing related communication assisting technologies such as amplify-and-forward (AF) relays, IRSs require much less energy consumption. Therefore, IRS-aided communication has been considered as a promising effective and green solution in future wireless communication.

Non-orthogonal multiple access (NOMA) is one of the key technologies in next-generation wireless communication networks due to its higher spectral efficiency achievement, user fairness guarantee, and massive connectivity support [4,5]. The key idea of NOMA is to serve multiple users in the same resource block (i.e., time, frequency and code), where superposition coding (SC) and successive interference cancellation (SIC) are applied at the transmitter and receiver, respectively [6,7]. Specifically, users who have better channel conditions can remove the intra-channel interference. In the current literatures, the performance gains of NOMA over orthogonal multiple access (OMA) have been investigated in various scenarios, such as cognitive radio [8] and millimeter wave communication [9]. Sparked by the aforementioned benefits of the IRS and NOMA, we explore in this paper the potential performance improvement brought by effective integration NOMA technology with IRS-aided communication.

A. Prior Works

1) *Studies on Single-Input Single-Output (SISO)-NOMA Systems*: Prior works on NOMA in the single-antenna scenario have studied various aspects such as user fairness, user grouping schemes, power allocation design, etc. For example, Timotheou *et al.* [10] studied the power allocation problem with the aim of guaranteeing fairness among served users. Ding *et al.* [11] further analyzed the performance of NOMA in both a fixed power allocation system (F-NOMA) and cognitive radio inspired NOMA (CR-NOMA) under different user pairing schemes. Choi *et al.* [12] proposed optimal power allocation schemes in a two-user downlink NOMA system, where the max-sum rate and max-min rate with proportional fairness objective functions were considered. A dynamic power allocation scheme (D-NOMA) for both downlink and uplink transmission was proposed by Yang *et al.* [13] while satisfying different users' quality of service (QoS) requirements, which demonstrated that D-NOMA outperforms F-NOMA and CR-NOMA

in terms of communication rate and fairness. Moreover, Liu *et al.* [14] studied cooperative NOMA with simultaneous wireless information and power transfer (SWIPT) technology, where near users with energy harvesting act as relays to enhance the received signal quality of far users. Fang *et al.* [15] studied multi-subcarrier downlink NOMA to maximize the energy efficiency by jointly optimizing subchannel assignment and power allocation, where a low complexity algorithm was designed based on matching theory and DC programming method. Full-duplex multi-subcarrier systems were investigated by Sun *et al.* [16], where the optimal power allocation and user scheduling scheme was designed by applying monotonic optimization theory.

2) *Studies on Multiple-Input Multiple-Output (MIMO)-NOMA Systems:* Hanif *et al.* [17] proposed an effective beamforming design algorithm to maximize the system sum rate, where a multi-antenna base station (BS) served multiple single-antenna users through the NOMA protocol. Considering multiple antenna techniques at both the BS and users, Ding *et al.* [18] studied the precoding and detection designs, where users are partitioned into several clusters and NOMA transmission was applied in each cluster. User fairness in MIMO-NOMA systems was investigated by Liu *et al.* [19], where three user clustering schemes with power allocation designs were proposed to guarantee user fairness with a lower computation complexity. Furthermore, a general framework for MIMO-NOMA in both downlink and uplink transmission was proposed in [20]. By adopting the signal alignment technique, the MIMO-NOMA transmission can be divided into several independent single-antenna cases for NOMA implementations. Ali *et al.* [21] optimized user scheduling, beamforming vectors and power allocation in multiuser MIMO-NOMA networks, where zero-forcing beamforming was designed with the equivalent channel gain of each cluster in order to cancel the inter-cluster interference. To investigate secure NOMA transmission, Liu *et al.* [22] analyzed the secrecy performance with stochastic geometry in both single-antenna and multiple-antenna scenarios. Particularly, artificial noise was invoked to enhance secrecy performance in multiple-antenna NOMA communication. Alavi *et al.* [23] investigated beamforming design with different objective functions based on perfect and imperfect channel state information (CSI). To further investigate the application of MIMO-NOMA, Ding *et al.* [24] proposed a precoding design scheme for Internet of Things (IoT) transmission scenarios. Wang *et al.* [25] applied NOMA to millimeter-wave communication with the concept of beamspace MIMO, which demonstrated that NOMA can achieve higher system spectrum and energy efficiency than the conventional beamspace MIMO communication.

3) *Studies on IRS-aided Systems:* In contrast to conventional communication systems, the channel response can be modified by deploying an IRS. Driven by this unique characteristic, some initial studies showed how to enhance system performance by designing the passive beamforming at the IRS. Wu *et al.* [26] developed iterative algorithms for beamforming design at both the BS and IRS to minimize the total transmit power. Chen [27] invoked IRSs for secure transmission in a downlink multiple-input single-output (MISO) system coexisting with multiple eavesdroppers. Cui *et al.* [28] further revealed that secure transmission can still be achieved with IRSs even when the eavesdropping channel is stronger than the legitimate channel. Furthermore, a novel IRS-aided NOMA communication model was proposed in [29], where IRSs were deployed at cell edge regions to maximize the total number of served users. Yang *et al.* [30] investigated the max-min rate problem in the SISO IRS-NOMA system, which showed that the spectrum efficiency gain of NOMA can be achieved even when the channel strengths of users are similar. Fu *et al.* [31] studied the total transmit power minimization problem in the downlink MISO NOMA IRS-aided system, where a penalty-based iterative algorithm was proposed to find the optimized beamforming vectors. Discrete phase shifters were considered in [32] and [33] when dealing with the transmit power minimization problem and weight sum-rate maximization problem in IRS-aided systems.

B. Motivation and Contributions

It is known that the success of SIC based detection at the users in NOMA transmission is mainly determined by the channel gains of different users. However, in IRS-aided systems, the channel response can be artificially modified by adjusting the reflection coefficients, which presents new challenges to the application of NOMA. Although few works investigated IRS-NOMA systems [29–31], to the best of our knowledge, there is no existing work on the sum rate optimization problem in the MISO IRS-NOMA system. The main challenges are as follows: i) for multi-antenna NOMA transmission, the decoding order is not determined by the users' channel gains order, since additional decoding rate conditions need to be satisfied to guarantee successful SIC [7]; ii) both the active and passive beamforming in IRS-NOMA affect the decoding order among users, which makes the decoding order design and beamforming design highly coupled.

Driven by the above challenges, in this article, we investigate the joint beamforming design at both the BS and IRS to maximize the sum rate in downlink MISO IRS-NOMA systems. Our main contributions of this paper are summarized as follows:

- We propose a downlink MISO IRS-NOMA framework, in which the IRS is utilized for spectrum efficiency enhancement. Based on the proposed framework, we formulate a joint active and passive beamforming design problem to maximize the system sum rate, subject to total transmit power, SIC decoding rate constraints, user rate fairness constraints and various constraints on IRS reflecting elements, which are defined as ideal and non-ideal IRS.
- For the ideal IRS, both the reflection amplitudes and phase shifts can be designed. We develop an iterative algorithm using alternating optimization (AO), where the non-convex active and passive beamforming design subproblems are alternatively solved by utilizing the successive convex approximation (SCA) technique. In addition, we prove that a rank-one solution can be always obtained for active beamforming design.
- For the non-ideal IRS, the reflection amplitudes are fixed with constant values and only phase shifts can be designed, including continuous phase shifters and discrete phase shifters. We first invoke a novel sequential rank-one constraint relaxation (SROCR) approach to deal with passive beamforming design problem with continuous phase shifters. In contrast to the conventional semidefinite relaxation (SDR), the proposed algorithm can find a locally optimal rank-one solution. Then, for discrete phase shifters, the passive beamforming is designed by leveraging the quantization method with some modifications.
- We show that the proposed algorithms are capable of achieving promising sum rate gains, compared to both the conventional system without the IRS and the IRS-OMA system. We also demonstrate that the performance gap between the 3-bit phase shifters and the ideal IRS is negligible.

C. Organization and Notations

The rest of this paper is organized as follows. Section II presents the system model and problem formulation. In Section III and Section IV, we propose efficient algorithms for the active and passive beamforming design under ideal and non-ideal IRS assumptions. Section V presents the numerical results to validate the effectiveness of our proposed designs. Finally, Section VI concludes the paper.

Notations: Scalars are denoted by lower-case letters. Vectors and matrices are denoted by bold-face lower-case and upper-case letters, respectively. $\mathbb{R}^{N \times M}$ and $\mathbb{C}^{N \times M}$ denote the space of $N \times M$ real-valued and complex-valued matrices, respectively. \mathbb{H}^N denotes the set of all N -dimensional

complex Hermitian matrices. \mathbb{S}^N denotes the set of all N -dimensional real symmetric matrices. \mathbf{I}_N represents an $N \times N$ identity matrix. $\text{rank}(\mathbf{A})$ and $\text{Tr}(\mathbf{A})$ denote the rank and the trace of matrix \mathbf{A} . $\mathbf{A} \succeq 0$ represents \mathbf{A} is a positive semidefinite matrix. \mathbf{a}^T , \mathbf{a}^H and $\text{diag}(\mathbf{a})$ denote the transpose, the conjugate transpose and the diagonal matrix of vector \mathbf{a} , respectively. $\text{Re}(\cdot)$ extracts the real value of a complex variable.

II. SYSTEM MODEL AND PROBLEM FORMULATION

A. System Model

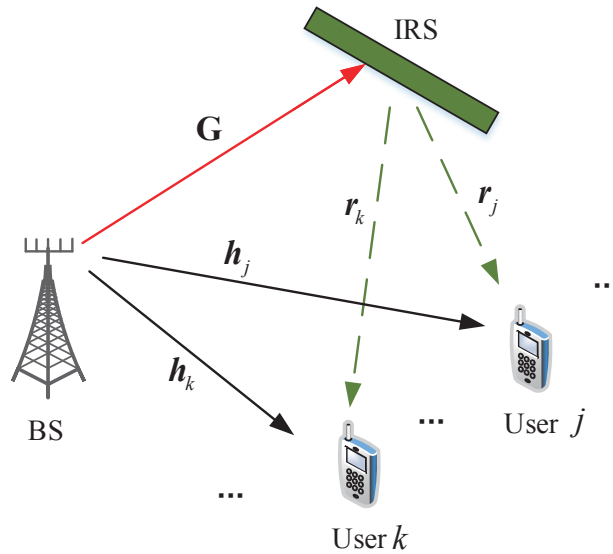


Fig. 1: Illustration of the downlink MISO IRS-NOMA system.

As shown in Fig. 1, we consider a downlink MISO IRS-NOMA system, which consists of an N -antenna base station, K single-antenna users and an IRS with M passive reflecting elements. In practice, the IRS is managed by the BS through a smart controller which exchanges information and coordinates transmission. Due to the severe path loss, we ignore the power of signals which are reflected by the IRS two or more times. To characterize the optimal performance of the IRS-NOMA system, it is assumed that the CSI of all channels involved are perfectly known at the BS. In addition, the quasi-static flat-fading model is adopted for all channels. Let $\Theta = \text{diag}(\mathbf{u}) \in \mathbb{C}^{M \times M}$ denote the diagonal reflection coefficients matrix of the IRS with $\mathbf{u} = [u_1, u_2, \dots, u_M]$ and $u_m = \beta_m e^{j\theta_m}$, where $\beta_m \in [0, 1]$ and $\theta_m \in [0, 2\pi)$ denote the reflection amplitude and phase shift of the m th reflecting element on the IRS, respectively. Depending on

the amplitude and phase shift features of reflecting elements, two sets of IRS assumptions are considered as follows [34]:

- **Ideal IRS:** In this scenario, the reflecting elements can be optimized with arbitrary continuous amplitudes and phase shifts. Thus, the feasible set of u_m can be expressed as

$$\Phi_1 = \{u_m \mid |u_m|^2 \in [0, 1]\}. \quad (1)$$

- **Non-ideal IRS:** In this scenario, the reflection amplitude is fixed with a constant value, such as $\beta_m = 1$. We further discuss the two scenarios of continuous phase shifters and discrete phase shifters. In particular, the feasible set of u_m for continuous phase shifters can be expressed as

$$\Phi_2 = \{u_m \mid u_m = e^{j\theta_m}, \theta_m \in [0, 2\pi)\}. \quad (2)$$

and the feasible set of u_m for discrete phase shifters with B resolution bits can be expressed as

$$\Phi_3 = \{u_m \mid |u_m|^2 = 1, \theta_m \in \mathcal{D}\}, \quad (3)$$

where $\mathcal{D} = \{\frac{n2\pi}{2^B}, n = 0, 1, 2, \dots, 2^B - 1\}$.

The baseband equivalent channels from the BS to user k , the IRS to user k and the BS to IRS are denoted by $\mathbf{h}_k \in \mathbb{C}^{N \times 1}$, $\mathbf{r}_k \in \mathbb{C}^{M \times 1}$ and $\mathbf{G} \in \mathbb{C}^{M \times N}$, respectively. We denote s_k and $\mathbf{w}_k \in \mathbb{C}^{N \times 1}$ as the information-bearing symbol and the beamforming vector for the k th user. Without loss of generality, signal s_k is assumed to have zero mean and unit variance, i.e., $\mathbb{E}[s_k s_k^H] = 1$. Therefore, the complex baseband signal transmitted from the BS can be expressed as $\mathbf{x} = \sum_{k=1}^K \mathbf{w}_k s_k$. Then, the received signal at user k can be expressed as

$$y_k = (\mathbf{h}_k^H + \mathbf{r}_k^H \Theta \mathbf{G}) \sum_{k=1}^K \mathbf{w}_k s_k + n_k, \quad (4)$$

where $n_k \sim \mathcal{CN}(0, \sigma^2)$ is the additive white Gaussian noise (AWGN) at user k with zero mean and variance σ^2 .

Based on the NOMA principle, each user tries to employ SIC to remove the intra-cell interference. In SISO NOMA systems, the optimal decoding order among users are determined by the channel gains. The user with a stronger channel gains can decode the user's signal who

has a weaker channel gains. However, this ordering method cannot be applied in a MISO NOMA system since the channel responses can be modified with the introduced IRS, which can change the decoding order to be any one of all the $K!$ different decoding orders. Let $\Omega(k)$ denote the decoding order of user k . For instance, if $\Omega(k) = i$, then user k is the i th signal to be decoded. Given any two users j and k satisfying $\Omega(k) < \Omega(j)$, the signal-to-interference-plus-noise ratio (SINR) of user j to decode user k is given by

$$\text{SINR}_{k \rightarrow j} = \frac{|(\mathbf{h}_j^H + \mathbf{r}_j^H \Theta \mathbf{G}) \mathbf{w}_k|^2}{\sum_{\Omega(i) > \Omega(k)} |(\mathbf{h}_j^H + \mathbf{r}_j^H \Theta \mathbf{G}) \mathbf{w}_i|^2 + \sigma^2}. \quad (5)$$

The corresponding decoding rate is $R_{j \rightarrow k} = \log_2(1 + \text{SINR}_{j \rightarrow k})$. The achievable SINR for user k can be expressed as

$$\text{SINR}_{k \rightarrow k} = \frac{|(\mathbf{h}_k^H + \mathbf{r}_k^H \Theta \mathbf{G}) \mathbf{w}_k|^2}{\sum_{\Omega(i) > \Omega(k)} |(\mathbf{h}_k^H + \mathbf{r}_k^H \Theta \mathbf{G}) \mathbf{w}_i|^2 + \sigma^2}. \quad (6)$$

The corresponding rate is $R_{k \rightarrow k} = \log_2(1 + \text{SINR}_{k \rightarrow k})$. Under the assumption of a given decoding order, to guarantee that SIC is performed successfully, the condition $R_{k \rightarrow j} \geq R_{k \rightarrow k}$ for $\Omega(j) > \Omega(k)$ should be satisfied. In addition, users with lower decoding order may not achieve an acceptable rate since most of transmit power can be allocated to users who have a higher decoding order. To guarantee rate fairness among the users, the following conditions should be satisfied with given decoding orders:

$$|(\mathbf{h}_k^H + \mathbf{r}_k^H \Theta \mathbf{G}) \mathbf{w}_{\Omega(i)}|^2 \leq |(\mathbf{h}_k^H + \mathbf{r}_k^H \Theta \mathbf{G}) \mathbf{w}_{\Omega(j)}|^2, \forall k, i, j \in \mathcal{K}, \Omega(i) > \Omega(j). \quad (7)$$

For example, let us consider the two users case. If the decoding order is set as $\Omega(k) = k, k = 1, 2$, then SIC decoding and rate fairness conditions can be expressed as

$$R_{1 \rightarrow 2} \geq R_{1 \rightarrow 1}, \quad (8a)$$

$$|(\mathbf{h}_k^H + \mathbf{r}_k^H \Theta \mathbf{G}) \mathbf{w}_2|^2 \leq |(\mathbf{h}_k^H + \mathbf{r}_k^H \Theta \mathbf{G}) \mathbf{w}_1|^2, k = 1, 2. \quad (8b)$$

For the three users case with the decoding order $\Omega(k) = k, k = 1, 2, 3$, the SIC decoding rate conditions at user 2 and user 3 and rate fairness condition among all users can be expressed as

$$R_{1 \rightarrow 2} \geq R_{1 \rightarrow 1}, R_{1 \rightarrow 3} \geq R_{1 \rightarrow 1}, R_{2 \rightarrow 3} \geq R_{2 \rightarrow 2}, \quad (9a)$$

$$|(\mathbf{h}_k^H + \mathbf{r}_k^H \Theta \mathbf{G}) \mathbf{w}_3|^2 \leq |(\mathbf{h}_k^H + \mathbf{r}_k^H \Theta \mathbf{G}) \mathbf{w}_2|^2 \leq |(\mathbf{h}_k^H + \mathbf{r}_k^H \Theta \mathbf{G}) \mathbf{w}_1|^2, k = 1, 2, 3. \quad (9b)$$

It is worth noting that when K users are served in the IRS-NOMA system, there will be $\frac{K(K-1)}{2}$ SIC decoding rate constraints and K^2 rate fairness constraints, which depend on not only the active beamforming coefficients $\{\mathbf{w}_k\}$ at the BS, but also the combined channel (which depends on the passive beamforming vector Θ at the IRS).

B. Problem Formulation

Our goal is to maximize the sum rate of all users by jointly optimizing the active beamforming coefficients $\{\mathbf{w}_k\}$ at the BS and the passive beamforming vector Θ at the IRS, subject to the total power constraint, the SIC decoding rate and the user rate fairness constraints under different IRS assumptions. The optimization problem can be formulated as

$$(P1) : \max_{\Omega, \Theta, \{\mathbf{w}_k\}} \sum_{k=1}^K R_{k \rightarrow k} \quad (10a)$$

$$\text{s.t. } R_{k \rightarrow j} \geq R_{k \rightarrow k}, \Omega(j) > \Omega(k), \quad (10b)$$

$$\sum_{k=1}^K \|\mathbf{w}_k\|^2 \leq P_T \quad (10c)$$

$$u_m \in \Phi, \quad (10d)$$

$$\Omega \in \Pi, \quad (10e)$$

$$(7). \quad (10f)$$

where Π denotes the set of all $K!$ possible SIC decoding orders and P_T denotes the total transmit power. Constraint (10b) guarantees that the SIC can be performed successfully. Constraint (10c) is the total transmission power constraint and constraint (10d) represents the considered IRS assumption. Constraint (10f) guarantees rate fairness among all users. However, Problem (P1) is a highly-coupled non-convex problem even with convex set Φ_1 , which makes it hard to find the global optimal solution. In the following, we propose efficient algorithms based on the AO method to find a near optimal solution.

III. IDEAL IRS CASE

In this section, we focus on the Problem (P1) with the ideal IRS. Before solving this problem, we first transform (P1) into a more tractable form. Let $\mathbf{H}_k = \begin{bmatrix} \text{diag}(\mathbf{r}_k^H) \mathbf{G} \\ \mathbf{h}_k^H \end{bmatrix}$ and $\mathbf{v} = [\mathbf{u} \ 1]^H$. Then, we have $|(\mathbf{h}_k^H + \mathbf{r}_k^H \Theta \mathbf{G}) \mathbf{w}_k|^2 = |\mathbf{v}^H \mathbf{H}_k \mathbf{w}_k|^2$. Furthermore, we introduce slack variables $\{S_{kj}\}$ and $\{I_{kj}\}$ such that

$$\frac{1}{S_{kj}} = |\mathbf{v}^H \mathbf{H}_j \mathbf{w}_k|^2, \quad (11)$$

$$I_{kj} = \sum_{\Omega(i) > \Omega(k)} |\mathbf{v}^H \mathbf{H}_j \mathbf{w}_i|^2 + \sigma^2, \quad (12)$$

Then, the decoding rate $R_{k \rightarrow j}$ can be expressed as

$$R_{k \rightarrow j} = \log_2 \left(1 + \frac{1}{S_{kj} I_{kj}} \right), \Omega(k) \leq \Omega(j). \quad (13)$$

With the above variable definitions, Problem (P1) can be transformed into

$$(P2) : \max_{\mathbf{v}, \{\mathbf{w}_k, R_{k \rightarrow j}, S_{kj}, I_{kj}\}} \sum_{k=1}^K R_{k \rightarrow k} \quad (14a)$$

$$\text{s.t. } R_{k \rightarrow j} \leq \log_2 \left(1 + \frac{1}{S_{kj} I_{kj}} \right), \Omega(k) \leq \Omega(j), \forall k, j \in \mathcal{K} \quad (14b)$$

$$\frac{1}{S_{kj}} \leq |\mathbf{v}^H \mathbf{H}_j \mathbf{w}_k|^2, \forall k, j \in \mathcal{K}, \quad (14c)$$

$$I_{jk} \geq \sum_{\Omega(i) > \Omega(k)} |\mathbf{v}^H \mathbf{H}_j \mathbf{w}_i|^2 + \sigma^2, \forall k, j \in \mathcal{K}, \quad (14d)$$

$$R_{k \rightarrow j} \geq \log_2 \left(1 + \frac{1}{S_{kk} I_{kk}} \right), \Omega(j) > \Omega(k), \forall k, j \in \mathcal{K}, \quad (14e)$$

$$|\mathbf{v}^H \mathbf{H}_j \mathbf{w}_k|^2 \geq |\mathbf{v}^H \mathbf{H}_j \mathbf{w}_i|^2, \Omega(k) < \Omega(i), \forall i, j, k, \quad (14f)$$

$$(10c) - (10e). \quad (14g)$$

Proposition 1. Problem (P2) is equivalent to Problem (P1).

Proof. Without loss of optimality to Problem (P1), constraints (14b), (14c) and (14d) can be met with equality. Specifically, when $k = j$, assume that any of the constraints in (14b) is satisfied with strict inequality, then we can always increase $R_{k \rightarrow j}$ to make the constraint (14b) satisfied

with equality while increasing the objective function's value. Furthermore, suppose that (14c) and (14d) are satisfied with strict inequality, then we can always reduce S_{kj} or increase I_{kj} to make all constraints satisfied with equality, which in turn increases the value of the RHS in (14b) and increases the objective function's value. When $k \neq j$, assume that any of the constraints in (14b) is satisfied with strict inequality, then we can always increase $R_{k \rightarrow j}$ without changing the objective function's value of (P1). Therefore, Problem (P2) is equivalent to Problem (P1). \square

However, Problem (P2) is still a non-convex problem since the decoding order Ω , the active beamforming coefficients $\{\mathbf{w}_k\}$ and the passive beamforming vector \mathbf{v} are highly-coupled. Since the total number of decoding order combinations is a finite value, the optimal sum rate can be obtained by solving Problem (P2) with any one of decoding orders at first and selecting the maximum objective function's value among all decoding orders. For a given decoding order, the sum rate maximization problem in (P2) with the ideal IRS is reduced to

$$(P3) : \max_{\mathbf{v}, \{R_{k \rightarrow j}, S_{kj}, I_{kj}\}} \sum_{k=1}^K R_{k \rightarrow k} \quad (15a)$$

$$\text{s.t. } 0 \leq |v_m|^2 \leq 1, m = 1, 2, \dots, M, v_{M+1} = 1, \quad (15b)$$

$$(10c), (14b) - (14f). \quad (15c)$$

In order to tackle the highly-coupled non-convex terms in Problem (P3), we decompose the original problem into the two subproblems of active beamforming optimization and passive beamforming optimization, which can be efficiently solved by the SCA technique as described next.

A. Active Beamforming Optimization

Define $\mathbf{W}_k = \mathbf{w}_k \mathbf{w}_k^H, \forall k$, which needs to satisfy $\mathbf{W}_k \succeq 0$ and $\text{rank}(\mathbf{W}_k) = 1$. Under any given feasible passive beamforming vector \mathbf{v} , the active beamforming optimization problem can be written as

$$(P3.1) : \max_{\{\mathbf{W}_k, R_{k \rightarrow j}, S_{kj}, I_{kj}\}} \sum_{k=1}^K R_{k \rightarrow k} \quad (16a)$$

$$\text{s.t. } \frac{1}{S_{kj}} \leq \text{Tr}(\mathbf{W}_k \mathbf{H}_j^H \mathbf{v} \mathbf{v}^H \mathbf{H}_j), \forall k, j \in \mathcal{K}, \quad (16b)$$

$$I_{kj} \geq \sum_{\Omega(i) > \Omega(k)} \text{Tr}(\mathbf{W}_i \mathbf{H}_j^H \mathbf{v} \mathbf{v}^H \mathbf{H}_j) + \sigma^2, \forall k, j \in \mathcal{K}, \quad (16c)$$

$$\text{Tr}(\mathbf{W}_k \mathbf{H}_j^H \mathbf{v} \mathbf{v}^H \mathbf{H}_j) \geq \text{Tr}(\mathbf{W}_i \mathbf{H}_j^H \mathbf{v} \mathbf{v}^H \mathbf{H}_j), \Omega(k) < \Omega(i), \forall i, j, k, \quad (16d)$$

$$\sum_{k=1}^K \text{Tr}(\mathbf{W}_k) \leq P_T, \quad (16e)$$

$$\mathbf{W}_k \succeq 0, \mathbf{W}_k \in \mathbb{H}^N, \forall k, \quad (16f)$$

$$\text{rank}(\mathbf{W}_k) = 1, \forall k, \quad (16g)$$

$$(14b), (14e). \quad (16h)$$

Lemma 1. For $x > 0$ and $y > 0$, $f(x, y) = \log_2\left(1 + \frac{1}{xy}\right)$ is a convex function with respect to x and y .

Proof. It is easy to prove lemma 1 by showing that the Hessian matrix of function $f(x, y)$ is positive semidefinite when $x > 0$ and $y > 0$. As a result, $f(x, y)$ is a convex function. \square

Problem (P3.1) is a non-convex problem due to the non-convex constraints (14b) and (16g). Based on lemma 1, the right hand side (RHS) of (14b) is a joint convex function with respect to S_{kj} and I_{kj} . By applying the first-order Taylor expansion, the lower bound at given local points $\{S_{kj}^l, I_{kj}^l\}$ can be expressed as

$$\log_2\left(1 + \frac{1}{S_{kj} I_{kj}}\right) \geq R_{kj}^{low} = \log_2\left(1 + \frac{1}{S_{kj}^l I_{kj}^l}\right) - \frac{(\log_2 e)(S_{kj} - S_{kj}^l)}{S_{kj}^l + S_{kj}^2 I_{kj}^l} - \frac{(\log_2 e)(I_{kj} - I_{kj}^l)}{I_{kj}^l + I_{kj}^2 S_{kj}^l}. \quad (17)$$

Then, Problem (P3.1) is approximated as the following problem

$$(P3.2) : \max_{\{\mathbf{W}_k, R_{k \rightarrow j}, S_{kj}, I_{kj}\}} \sum_{k=1}^K R_{k \rightarrow k} \quad (18a)$$

$$\text{s.t. } R_{k \rightarrow j} \leq R_{kj}^{low}, \forall k, j \in \mathcal{K}, \quad (18b)$$

$$(14e), (16b) - (16g). \quad (18c)$$

Note that the remaining non-convexity of (P3.2) is the rank-one constraint (16g). To tackle this issue, we have the following theorem:

Theorem 1. Without loss of optimality, the obtained solution to Problem (P3.2) without rank-one constraint (16g) can always satisfy $\text{rank}(\mathbf{W}_k) \leq 1, \forall k \in \mathcal{K}$.

Proof. See Appendix A. \square

Based on Theorem 1, we can always obtain a rank-one solution by solving (P3.2) by ignoring the rank-one constraint (16g). As a result, the relaxed problem is a convex semidefinite program (SDP), which can be efficiently solved via standard convex problem solvers such as CVX [35]. It is worth noting that the objective function's value obtained from Problem (P3.2) in general provides a lower bound on that of Problem (P3.1). After solving (P3.2), the active beamforming coefficients $\{\mathbf{w}_k\}$ can be obtained through Cholesky decomposition, e.g. $\mathbf{W}_k^* = \mathbf{w}_k \mathbf{w}_k^H, \forall k$.

B. Passive Beamforming Optimization with Φ_1

Given any feasible active beamforming vectors $\{\mathbf{w}_k\}$, the passive beamforming optimization problem with ideal IRS can be written as

$$(P3.3) : \max_{\mathbf{v}, \{R_{k \rightarrow j}, S_{kj}, I_{kj}\}} \sum_{k=1}^K R_{k \rightarrow k} \quad (19a)$$

$$\text{s.t. (14b) - (14f), (15b).} \quad (19b)$$

Problem (P3.3) is a non-convex problem due to non-convex constraints (14b), (14c) and (14f). In the previous subsection, we have already showed how to tackle the non-convex constraint (14b). For the non-convex constraint (14c), the RHS is a convex function with respect to \mathbf{v} , the lower bound with the first-order Taylor expansion at the given local point $\mathbf{v}^{(l)}$ can be expressed as

$$|\mathbf{v}^H \mathbf{H}_j \mathbf{w}_k|^2 \geq \lambda_{kj} = \left| \mathbf{v}^{(l)H} \mathbf{H}_j \mathbf{w}_k \right|^2 + 2 \operatorname{Re} \left(\left(\mathbf{v}^{(l)H} \mathbf{H}_j \mathbf{w}_k \mathbf{w}_k^H \mathbf{H}_j^H \right) (\mathbf{v} - \mathbf{v}^{(l)}) \right). \quad (20)$$

Similarly, for the non-convex constraint (14f), the left hand side (LHS) can be replaced with the lower bound in (20). Then, the passive beamforming optimization problem is approximated as the following problem

$$(P3.4) : \max_{\mathbf{v}, \{R_{kj}, S_{kj}, I_{kj}\}} \sum_{k=1}^K R_{k \rightarrow k} \quad (21a)$$

$$\text{s.t. } R_{j \rightarrow k} \leq R_{jk}^{\text{low}}, \forall k, j \in \mathcal{K}, \quad (21b)$$

$$\frac{1}{S_{jk}} \leq \lambda_{kj}, \quad (21c)$$

$$\lambda_{kj} \geq |\mathbf{v}^H \mathbf{H}_j \mathbf{w}_i|^2, \Omega(k) < \Omega(i), \forall i, j, k, \quad (21d)$$

$$(14d), (14e), (15b). \quad (21e)$$

Algorithm 1 Proposed SCA-based algorithm for solving Problem (P3) with Φ_1

Initialize a decoding order Ω and feasible solutions $\{\mathbf{w}_k^l\}, \mathbf{v}^l$ to (P3), $l = 0$.

1: **repeat**

2: Solve Problem (P3.2) for given \mathbf{v}^l , and denote the optimal solutions as $\{\mathbf{w}_k^{l+1}\}$.

3: Solve Problem (P3.4) for given $\{\mathbf{w}_k^{l+1}\}$, and denote the optimal solution as \mathbf{v}^{l+1} .

4: $l = l + 1$.

5: **until** the fractional decrease of the objective value is below a threshold $\xi > 0$.

Now, it is easy to verify that Problem (P3.4) is a convex problem, which can be efficiently solved via standard convex problem solvers such as CVX [35]. Similarly, the objective function's value obtained from (P3.4) serves as a lower bound on that of (P3.3).

C. Proposed Algorithm, Complexity and Convergence

Based on the two subproblems formulated in the previous subsections, we propose an iterative algorithm for Problem (P3) with the ideal IRS by utilizing the AO method. Specifically, the active beamforming coefficients $\{\mathbf{w}_k\}$ and the passive beamforming vector \mathbf{v} are alternately optimized by solving Problem (P3.2) and (P3.4), where the solutions obtained in each iteration are used as the input local points for the next iteration. The details of the proposed algorithm are summarized in **Algorithm 1**. The complexity of each subproblem with the interior-point method are $\mathcal{O}\left((3K^2 + N^2)^{3.5}\right)$ and $\mathcal{O}\left((3K^2 + M)^{3.5}\right)$. Then, the total complexity of Algorithm 1 is $\mathcal{O}\left(I_{ite}^l (6K^2 + N^2 + M)^{3.5}\right)$, where I_{ite}^l denotes the iteration number of Algorithm 1.

Next, we demonstrate the convergence of Algorithm 1. Define $\eta_{\Phi_1}(\{\mathbf{w}_k^l\}, \mathbf{v}^l)$ as the objective function's value of Problem (P3) in the l th iteration. First, for Problem (P3.2) with given passive beamforming vector in step 2 of Algorithm 1, we have

$$\begin{aligned} \eta_{\Phi_1}(\{\mathbf{w}_k^l\}, \mathbf{v}^l) &\stackrel{(a)}{=} \eta_{\mathbf{w}}^{lb}(\{\mathbf{w}_k^l\}, \mathbf{v}^l) \\ &\stackrel{(b)}{\leq} \eta_{\mathbf{w}}^{lb}(\{\mathbf{w}_k^{l+1}\}, \mathbf{v}^l) \\ &\stackrel{(c)}{\leq} \eta_{\Phi_1}(\{\mathbf{w}_k^{l+1}\}, \mathbf{v}^l), \end{aligned} \tag{22}$$

where $\eta_{\mathbf{w}}^{lb}$ represents the objective function's value of Problem (P3.2). (a) follows the fact that the first-order Taylor expansions are tight at the given local points in Problem (P3.2); (b) holds since Problem (P3.2) is solved optimally; (c) holds due to the fact that the objective function's value of Problem (P3.2) serves as a lower bound on that of (P3.1). This suggests that the objective function's value of Problem (P3.1) is non-decreasing in each iteration.

Similarly, for Problem (P3.4) with given active beamforming coefficients in step 3 of Algorithm 1, we have

$$\begin{aligned} \eta_{\Phi_1}(\{\mathbf{w}_k^{l+1}\}, \mathbf{v}^l) &\stackrel{(a)}{=} \eta_{\mathbf{v}}^{lb}(\{\mathbf{w}_k^{l+1}\}, \mathbf{v}^l) \\ &\stackrel{(b)}{\leq} \eta_{\mathbf{v}}^{lb}(\{\mathbf{w}_k^{l+1}\}, \mathbf{v}^{l+1}) \\ &\stackrel{(c)}{\leq} \eta_{\Phi_1}(\{\mathbf{w}_k^{l+1}\}, \mathbf{v}^{l+1}), \end{aligned} \quad (23)$$

where $\eta_{\mathbf{v}}^{lb}$ represents the objective function's value of Problem (P3.4).

As a result, based on (22) and (23), we obtain that

$$\eta_{\Phi_1}(\{\mathbf{w}_k^l\}, \mathbf{v}^l) \leq \eta_{\Phi_1}(\{\mathbf{w}_k^{l+1}\}, \mathbf{v}^{l+1}). \quad (24)$$

Remark 1. Equation (24) indicates that the objective function's value of Problem (P3) is non-decreasing after each iteration. Since the system sum rate is upper bounded by a finite value, the proposed algorithm is guaranteed to converge to a locally optimal solution of Problem (P3).

IV. NON-IDEAL IRS CASE

In this section, we solve Problem (P2) with non-ideal IRS. The sum rate maximization problem in (P2) with a given decoding order can be written as

$$(P4) : \quad \max_{\mathbf{v}, \{\mathbf{w}_k, R_{k \rightarrow j}, S_{kj}, I_{kj}\}} \sum_{k=1}^K R_{k \rightarrow k} \quad (25a)$$

$$\text{s.t. } v_m \in \Phi_2 \text{ or } \Phi_3, m = 1, 2, \dots, M, v_{M+1} = 1, \quad (25b)$$

$$(10c), (14b) - (14f). \quad (25c)$$

To tackle this problem, we still decompose (P4) into two subproblems. Fortunately, the active beamforming coefficients can be still optimized by solving (P3.2). We only need to focus on how to optimize the passive beamforming vector with the case of Φ_2 or Φ_3 . In the following, we first invoke a novel SROCR approach [36] to deal with the passive beamforming optimization with continuous phase shifters. Then, the passive beamforming design for discrete phase shifters is handled with the quantization-based scheme.

A. Passive Beamforming Optimization with Φ_2

Equipped with continuous phase shifters, each element on the IRS has a constant reflection amplitude, i.e. $|v_m|^2 = 1$. To tackle the unit modulus constraint, we define $\mathbf{V} = \mathbf{v}\mathbf{v}^H$ which satisfies $\mathbf{V} \succeq 0$, $\text{rank}(\mathbf{V}) = 1$ and $[\mathbf{V}]_{mm} = 1, m = 1, 2, \dots, M + 1$. Then, under any given feasible active beamforming coefficients $\{\mathbf{w}_k^l\}$, Problem (P4) can be written as

$$(P4.1) : \max_{\mathbf{V}, \{R_{k \rightarrow j}, S_{kj}, I_{kj}\}} \sum_{k=1}^K R_{k \rightarrow k} \quad (26a)$$

$$\text{s.t. } \frac{1}{S_{kj}} \leq \text{Tr}(\mathbf{V}\mathbf{H}_j \mathbf{w}_k \mathbf{w}_k^H \mathbf{H}_j^H), \forall k, j \in \mathcal{K}, \quad (26b)$$

$$I_{kj} \geq \sum_{\Omega(i) > \Omega(k)} \text{Tr}(\mathbf{V}\mathbf{H}_j \mathbf{w}_i \mathbf{w}_i^H \mathbf{H}_j^H) + \sigma^2, \forall k, j \in \mathcal{K}, \quad (26c)$$

$$\text{Tr}(\mathbf{V}\mathbf{H}_j \mathbf{w}_k \mathbf{w}_k^H \mathbf{H}_j^H) \geq \text{Tr}(\mathbf{V}\mathbf{H}_j \mathbf{w}_i \mathbf{w}_i^H \mathbf{H}_j^H), \Omega(k) < \Omega(i), \forall i, j, k, \quad (26d)$$

$$[\mathbf{V}]_{mm} = 1, m = 1, 2, \dots, M + 1, \quad (26e)$$

$$\mathbf{V} \succeq 0, \mathbf{V} \in \mathbb{H}^{M+1}, \quad (26f)$$

$$\text{rank}(\mathbf{V}) = 1, \quad (26g)$$

$$(14b), (14e). \quad (26h)$$

The non-convexity of (P4.2) lies in the non-convex constraint (14b) and the rank-one constraint (26g). Similarly, the non-convex constraint can be replaced with its lower bound in (17). For the rank-one constraint (26g), the conventional approach is applying semidefinite relaxation (SDR) [26], where we first solve the problem by ignoring the rank-one constraint, and then construct a rank-one solution with Gaussian randomization method if the solution obtained from the relaxed problem is not rank-one. One drawback of this approach is that the constructed rank-one solution is normally a suboptimal solution or even infeasible for the original problem. The objective function's value may not be non-increasing in each iteration, which results in the convergence of the proposed algorithm can not be guaranteed. Driven by this issue, we propose a novel SROCR-based algorithm to obtain a local optimal rank-one solution. The basic framework of the SROCR approach can be found in Appendix B. By replacing the non-convex term in (14b) with the lower bound in (17), Problem (P4.1) can be written as

$$(P4.2) : \max_{\mathbf{V}, \{R_{k \rightarrow j}, S_{kj}, I_{kj}\}} \sum_{k=1}^K R_{k \rightarrow k} \quad (27a)$$

$$\text{s.t. } R_{j \rightarrow k} \leq R_{jk}^{\text{low}}, \forall k, j \in \mathcal{K}, \quad (27\text{b})$$

$$\text{rank}(\mathbf{V}) = 1, \quad (27\text{c})$$

$$(14\text{e}), (26\text{b}) - (26\text{f}). \quad (27\text{d})$$

Now, Problem (P4.2) satisfies the general framework for the SROCR approach, which is shown in Problem (P) in Appendix B. Therefore, we apply the SROCR approach to solve Problem (P4.2). First, we replace the non-convex rank-one constraint with the relaxed convex constraint which controls the largest eigenvalue to trace ratio of \mathbf{V} with the parameter $\omega^{(i)} \in [0, 1]$. Thus, the relaxed optimization problem can be expressed as

$$(P4.3) : \max_{\mathbf{V}, \{R_{k \rightarrow j}, S_{kj}, I_{kj}\}} \sum_{k=1}^K R_{k \rightarrow k} \quad (28\text{a})$$

$$\text{s.t. } u_{\max}(\mathbf{V}^{(i)})^H \mathbf{V} u_{\max}(\mathbf{V}^{(i)}) \geq \omega^{(i)} \text{Tr}(\mathbf{V}), \quad (28\text{b})$$

$$(14\text{e}), (26\text{b}) - (26\text{f}), (27\text{b}), \quad (28\text{c})$$

where $u_{\max}(\mathbf{V}^{(i)})$ is the eigenvector corresponding to the largest eigenvalue of $\mathbf{V}^{(i)}$ and $\mathbf{V}^{(i)}$ is the obtained solution in the i th iteration with $\omega^{(i)}$. It can be verified that Problem (P4.3) is a convex problem that can be efficiently solved with convex optimization software, such as CVX [35]. The parameter $\omega^{(i)}$ gradually increases from 0 to 1 in each iteration in order to obtain a locally optimal rank-one solution for (P4.2). The details of solving Problem (P4.2) are summarized in **Algorithm 2**. Similarly, the objective function's value obtained from (P4.2) serves as a lower bound on that of (P4.1) due to the replacement of non-convex terms with their lower bounds. After solving (P4.2), the passive beamforming vector \mathbf{v} for the continuous phase shifters case can be obtained through Cholesky decomposition, e.g. $\mathbf{V}^{l+1} = \mathbf{v}\mathbf{v}^H$.

B. Passive Beamforming Optimization with Φ_3

In this subsection, we discuss the passive beamforming design with discrete phase shifters. The optimization problem becomes a combinatorial optimization problem. Though the optimal solution can be obtained via an exhaustive search, it requires a prohibitive complexity since the number of elements on the IRS is usually large. Recall the fact that elements in Φ_2 and Φ_3 both must follow the unit modulus constraint. Hence, we can directly quantize the obtained solution \mathbf{v}_{Φ_2} in the continuous phase shifters case to the nearest feasible point \mathbf{v}_{Φ_3} in the discrete phase

Algorithm 2 Iterative algorithm for solving Problem (P4.2)

Initialize convergence thresholds ϵ_1 , ϵ_2 and feasible \mathbf{V}^l to problem (P4.2), $i = 0$.
 Solve the relaxed problem (P4.3) and obtain $\mathbf{V}^{(i)}$ when $\omega^{(i)} = 0$.
 Define an initial step size $\delta^{(i)}$.

- 1: **repeat**
 - 2: Given $\{\omega^{(i)}, \mathbf{V}^{(i)}\}$, solve the convex Problem (P4.3).
 - 3: **if** Problem (P4.3) is solvable **then**
 - 4: Define the optimal solution as $\mathbf{V}^{(i+1)}$,
 - 5: $\delta^{(i+1)} = \delta^{(i)}$;
 - 6: **else**
 - 7: $\delta^{(i+1)} = \delta^{(i)}/2$.
 - 8: **end**
 - 9: $\omega^{(i+1)} = \min \left(1, \frac{\lambda_{\max}(\mathbf{V}^{(i+1)})}{\text{Tr}(\mathbf{V}^{(i+1)})} + \delta^{(i+1)} \right)$.
 - 10: $i = i + 1$.
 - 11: **until** $\omega^{(i-1)} \geq \epsilon_1$ and $|g_0(\mathbf{X}^{(i)}) - g_0(\mathbf{X}^{(i-1)})| \leq \epsilon_2$, $\mathbf{V}^{l+1} = \mathbf{V}^{(i)}$.
-

shifters case as follows

$$v_{m,\Phi_3} = \begin{cases} e^{j\theta_m^*}, & m = 1, \dots, M, \\ 1, & m = M + 1, \end{cases} \quad (29)$$

where

$$\theta_m^* = \arg \min_{\theta \in \mathcal{D}} |\theta - \text{angle}(v_{m,\Phi_2})|.$$

However, the obtained solution \mathbf{v}_{Φ_3} with quantization method may not be a locally optimal solution. In order to make the objective function's value to be non-increasing in each iteration for Φ_3 , we update \mathbf{v}_{Φ_3} only when $\eta_{\Phi_3}(\{\mathbf{w}_k^{l+1}\}, \mathbf{v}_{\Phi_3}^{l+1}) \geq \eta_{\Phi_3}(\{\mathbf{w}_k^{l+1}\}, \mathbf{v}_{\Phi_3}^l)$.

C. Proposed Algorithm, Complexity and Convergence

Similarly, we propose an iterative algorithm for Problem (P4) with non-ideal IRS by utilizing the AO method. The details of the proposed algorithm are summarized in **Algorithm 3**. The complexity of the passive beamforming optimization with interior-point method is $\mathcal{O}\left(I_{ite}^S (3K^2 + M^2)^{3.5}\right)$, where I_{ite}^S denotes the iteration number of Algorithm 2 with the SROCR approach. The total complexity of Algorithm 3 is $\mathcal{O}\left(I_{ite}^N \left((3K^2 + N^2)^{3.5} + I_{ite}^S (3K^2 + M^2)^{3.5}\right)\right)$, where I_{ite}^N denotes the iteration number of Algorithm 3. It can be seen that complexity of the non-ideal IRS scenario is larger than that of the ideal IRS scenario. The convergence of Algorithm 3 can be addressed in a similar way as Algorithm 1.

Algorithm 3 Proposed SROCR-based algorithm for solving Problem (P4) with Φ_2 or Φ_3

Initialize a decoding order Ω and feasible solutions $\{\mathbf{w}_k^l\}$, \mathbf{v}^l to (P4), $l = 0$.

- 1: **repeat**
 - 2: Solve Problem (P3.2) for given \mathbf{v}^l , and denote the optimal solutions as $\{\mathbf{w}_k^{l+1}\}$.
 - 3: Solve Problem (P4.2) with the proposed Algorithm 2 for given $\{\mathbf{w}_k^{l+1}\}$, and denote the optimal solution as \mathbf{v}^{l+1} .
 - 4: **if** $\Phi = \Phi_3$ **then**
 - 5: Construct the feasible solution \mathbf{v}_{Φ_3} via (29) with \mathbf{v}^{l+1} .
 - 6: **if** $(\{\mathbf{w}_k^{l+1}\}, \mathbf{v}_{\Phi_3}^{l+1}) \geq \eta_{\Phi_3}(\{\mathbf{w}_k^{l+1}\}, \mathbf{v}_{\Phi_3}^l)$ **then**
 - 7: $\mathbf{v}^{l+1} = \mathbf{v}_{\Phi_3}$,
 - 8: **else**
 - 9: $\mathbf{v}^{l+1} = \mathbf{v}^l$.
 - 10: **end**
 - 11: **end**
 - 12: $l = l + 1$.
 - 13: **until** the fractional decrease of the objective value is below a threshold $\xi > 0$.
-

Remark 2. In practical applications, it is costly to deploy IRSs with ideal case or continuous phase shifters due to hardware limitations. However, it is still important to analyze the cases of Φ_1 and Φ_2 since they provide a theoretical performance upper bounds to the case of Φ_3 .

D. Passive Beamforming Optimization with 1-Bit Phase Shifters

As described earlier, the quantization method can provide a feasible solution for the passive beamforming design in the discrete phase shifters case. However, this method may experience substantial performance losses with low-resolution phase shifters, e.g., $B = 1$. To overcome this drawback, we investigate the passive beamforming design with 1-bit phase shifters in this subsection. Specifically, the passive beamforming optimization problem of 1-bit phase shifters under given $\{\mathbf{w}_k\}$ can be written as

$$(P4.4) : \max_{\mathbf{v}, \{R_{k \rightarrow j}, S_{kj}, I_{kj}\}} \sum_{k=1}^K R_{k \rightarrow k} \quad (30a)$$

$$\text{s.t. } v_m \in \{-1, 1\}, m = 1, 2, \dots, M, v_{M+1} = 1, \quad (30b)$$

$$(14b) - (14f). \quad (30c)$$

Problem (P4.4) is a Boolean quadratic problem (BQP). Similarly, let $\mathbf{V} = \mathbf{v}\mathbf{v}^H$ which satisfies $\mathbf{V} \in \mathbb{S}^{M+1}$, $\mathbf{V} \succeq 0$, $\text{rank}(\mathbf{V}) = 1$ and $[\mathbf{V}]_{mm} = 1, m = 1, 2, \dots, M + 1$. Then, Problem (P4.4)

can be expressed as

$$(P4.5) : \max_{\mathbf{V}, \{R_{k \rightarrow j}, S_{kj}, I_{kj}\}} \sum_{k=1}^K R_{k \rightarrow k} \quad (31a)$$

$$\text{s.t. } R_{j \rightarrow k} \leq R_{jk}^{low}, \forall k, j \in \mathcal{K}, \quad (31b)$$

$$\mathbf{V} \succeq 0, \mathbf{V} \in \mathbb{S}^{M+1}, \quad (31c)$$

$$\text{rank}(\mathbf{V}) = 1, \quad (31d)$$

$$(14e), (26b) - (26e). \quad (31e)$$

Problem (P4.5) can be regarded as a non-convex rank-one optimization problem with a real symmetric matrix set, which can also be solved by the proposed SROCR-based algorithm.

Remark 3. Since a locally optimal rank-one solution can be obtained for the passive beamforming optimization with the SROCR approach, the sum rate performance of 1-bit phase shifters obtained by the SROCR-based algorithm will be no worse than that of the quantization scheme.

V. SIMULATION RESULTS

In this section, simulation results are provided to validate the effectiveness of our proposed algorithms. As illustrated in Fig. 2, we consider a downlink MISO IRS-NOMA system, where the BS and IRS are located at $(0, 0, 0)$ and $(50, 0, 0)$, respectively. The served users are randomly distributed on a half circle centered at the BS or the IRS. We consider the case of two users, i.e., $K = 2$. The BS-user1 distance and the IRS-user2 distance are both set to 20m. The path loss model is given by $L(d) = C_0 d^{-\alpha}$, where C_0 denotes the path loss at the reference distance of 1 meter, d is the individual link distance and α denotes the path loss exponent. For small-scale fading, we assume a Rayleigh fading channel model for the BS-user and IRS-user channels and Rician fading model for the BS-IRS channel. The Rician factor is denoted as κ . We set the simulation parameters as follow: $C_0 = -30\text{dB}$, $\sigma^2 = -70\text{dBW}$, $\alpha_{BU} = 3.5$, $\alpha_{IU} = 2.8$, $\alpha_{BI} = 2.2$ and $\kappa = 3\text{dB}$. All simulation results are obtained by averaging over 100 independent channel realizations and the convergence threshold is $\xi = 10^{-2}$.

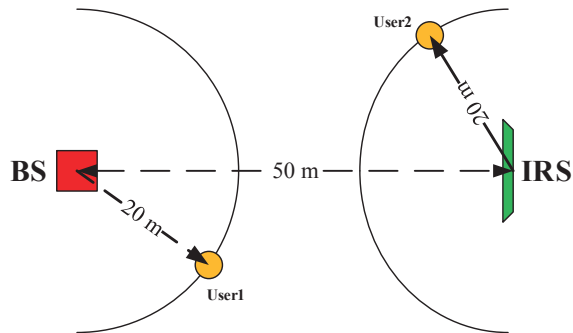


Fig. 2: Simulation setup of the MISO IRS-NOMA system (top view).

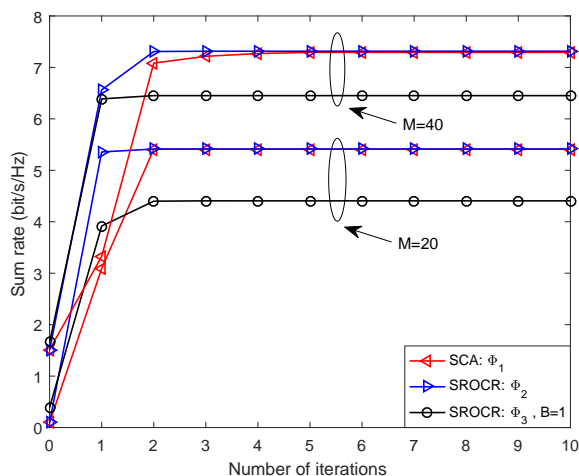


Fig. 3: The sum rate versus the number of iterations, $N = 2$, $K = 2$, $P_T = 10\text{dBm}$.

A. Convergence Performances of Proposed Algorithms

In Fig. 3, we first provide the convergence performances of Algorithm 1 and Algorithm 3 with $N = 2$ and $P_T = 10\text{dBm}$. The initial active beamforming coefficients $\{\mathbf{w}_k^0\}$ and passive beamforming vector \mathbf{v}^0 are obtained with the following method:

- **Passive beamforming initialization:** In the Φ_1 and Φ_2 cases, the phase shift of each element is uniformly distributed between $[0, 2\pi)$ and the reflection amplitude is set to 1. In the Φ_3 case, the initial passive beamforming vector is obtained by quantizing the random continuous phase shifts to the discrete phase shifts set.
- **Active beamforming initialization:** Given the initial passive beamforming vector, the active beamforming vectors are generated with equal power allocation $\frac{P_T}{K}$, while satisfying the SIC decoding rate conditions and user rate fairness constraints.

From Fig. 3, it is observed that the sum rate performances of proposed algorithms increase

quickly with the number of iterations and converge with around 5 iterations, which is consistent with **Lemma 1**.

B. Impact of the IRS

In order to demonstrate the benefits brought by the IRS, we compare our proposed algorithms with the following benchmark schemes:

- **Random phase shifts:** In this case, the phase shifts of IRS elements are set with random values in Φ_2 . Then, we only optimize the active beamforming at the BS with the combined channels by solving Problem (P3.2).
- **Without IRS:** In this case, the BS served multiple users without the aid of an IRS. The active beamforming vectors are optimized with BS-user channels by solving Problem (P3.2).

1) *Sum Rate versus Transmit Power:* Fig. 4 presents the achieved system sum rate versus the transmit power with different schemes when $N = 2$ and $M = 20$. It is observed that the sum rate performances of all considered schemes increase with the increase of P_T . The performances of our proposed algorithms significantly outperform the other two benchmark schemes. Furthermore, the performance gap between the schemes with the IRS and the “Without IRS” scheme becomes larger when the transmit power P_T increases, which indicates the advantages of the deployment of IRSs. We also observe that the sum rate performances of our proposed algorithms outperforms the “Random phase shifts” scheme whose reflection coefficients are not optimized. From the perspective of different IRS assumptions, it is observed that the performance gaps between the case of ideal IRS Φ_1 and continuous phase shifters Φ_2 can be ignored. This is because the amplitudes of the passive beamforming vectors obtained from Algorithm 1 are nearly 1. For practical discrete phase shifters Φ_3 , we observe that the performance degradation caused by finite resolution phase shifters decreases as the bit resolution increases. Moreover, the performance achieved by the SROCR-based algorithm in the 1-bit phase shifters case outperforms the quantization scheme, which is consistent with **Lemma 3**. This is because the SROCR-based algorithm can always find a locally optimal rank-one solution.

2) *Sum Rate versus the Number of IRS Elements:* In Fig. 5, we provide the sum rate performance versus the number of IRS elements M with $N = 2$ and $P_T = 10$ dBm for different schemes. It is observed that the sum rate performances of all IRS-NOMA schemes increase with the increase of M , while the sum rate performance of the system without the IRS remains unchanged. This is expected since a higher gain can be achieved with a larger number of IRS

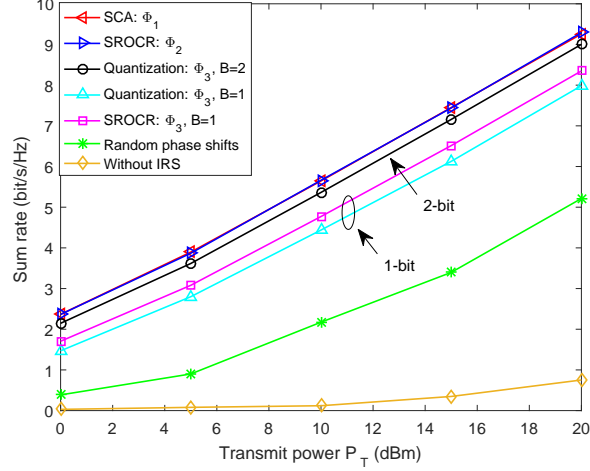


Fig. 4: The sum rate versus transmit power P_T , $N = 2$, $M = 20$, $K = 2$.

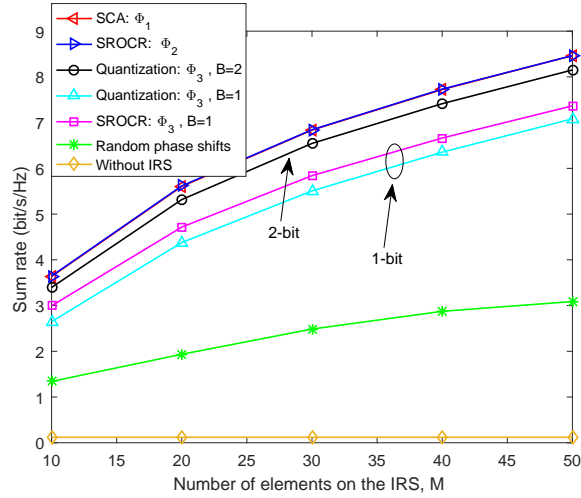


Fig. 5: The sum rate versus IRS element number M , $N = 2$, $K = 2$, $P_T = 10\text{dBm}$.

elements. In addition, the performance gap between the discrete phase shifters case and the ideal IRS case increases as M increases. This implies that more resolution bits are required when the number of IRS elements is large.

3) *Sum Rate versus the Resolution Bits*: Fig. 6 illustrates the sum rate performance versus the number of resolution bits of the IRS phase shifters. The ideal IRS case achieves the best performance, while the discrete case of Φ_3 achieves the worst performance. This is expected since $\Phi_1 \supseteq \Phi_2 \supseteq \Phi_3$, which is also consistent with **Lemma 2**. We also observe that the performance gap between Φ_3 and Φ_1 becomes narrower with the increase of resolution bits. As illustrated, “1-bit” and “2-bit” schemes can achieve 80% and 90% performance of the ideal IRS case, respectively. Moreover, the performance loss between the “3-bit” scheme and the ideal IRS is

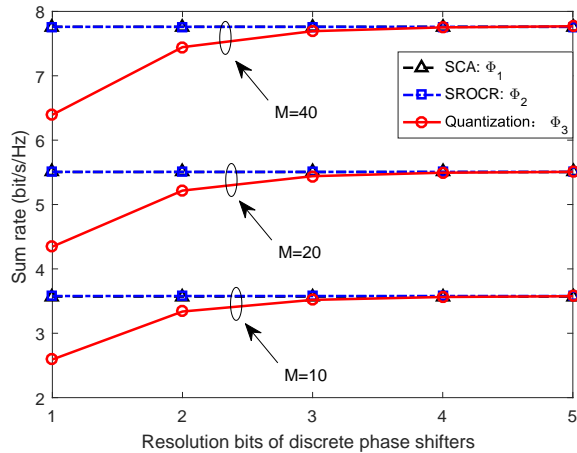


Fig. 6: The sum rate versus transmit power P_T , $N = 2$, $M = 20$, $K = 2$.

negligible.

C. Impact of Decoding Order

To evaluate the impact of the decoding order on the sum rate performance, we compare the following schemes: 1) “IRS-NOMA-Exhaust” denotes our proposed algorithms where the optimal decoding order is selected through exhaustive search; 2) “IRS-NOMA-Random” denotes the case where the active and passive beamforming vectors are optimized with a randomly selected decoding order. For both schemes, continuous phase shifters are assumed and $N = 2$. As illustrated in Fig. 7, our proposed algorithm significantly outperforms the benchmark scheme, which highlights the importance of finding the optimal decoding order. It is worth noting that our proposed algorithms need to search over $K!$ possible decoding orders, which is acceptable when the number of users is not large. However, when K is large, the complexity will be prohibitively high. In this case, some low-complexity ordering methods are required.

D. Performance Comparison with OMA

Finally, we compare our proposed IRS-NOMA scheme with the IRS-OMA scheme. In the IRS-OMA scheme, the BS serves all users through time division multiple access with the aid of the IRS, where the active and passive beamforming vectors are jointly optimized to maximize the received signal strength at the served user during each time slot. Fig. 8 depicts the sum rate performance of both IRS-NOMA and IRS-OMA schemes with $N = K = 2$ in the continuous phase shifters case. It is observed that the IRS-NOMA scheme significantly outperforms the

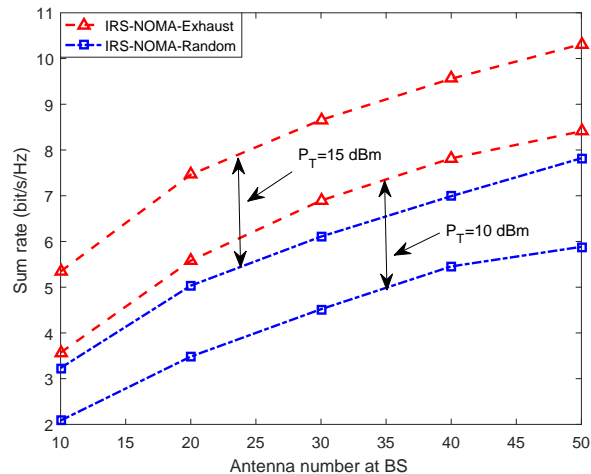


Fig. 7: The sum rate versus IRS element number M , $N = 2$, $K = 2$.

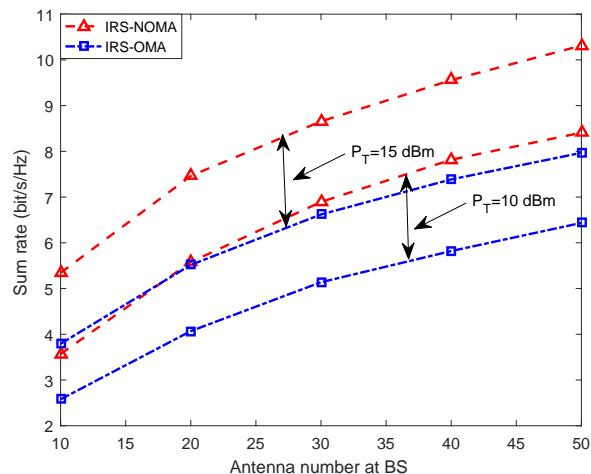


Fig. 8: The sum rate versus IRS element number M , $N = 2$, $K = 2$.

IRS-OMA scheme with more than 5 dB performance gain. This is expected since all users can be served simultaneously through the NOMA protocol compared with the OMA scheme.

VI. CONCLUSION

In this paper, the MISO IRS-NOMA system has been investigated. The sum rate maximization problem was formulated by jointly optimizing the active and passive beamforming vectors under various IRS elements assumptions. To tackle these non-convex problems, the original problem was decoupled into two subproblems, namely, active beamforming optimization and passive beamforming optimization. For the ideal IRS case, the two non-convex subproblems were alternately solved by applying the SCA technique. For the non-ideal IRS case, a novel

SROCR-based algorithm was proposed to find a locally optimal rank-one solution for continuous phase shifters. A quantization-based scheme was designed for discrete phase shifters. Moreover, our proposed algorithms were proved to be convergent. Numerical results showed the significant performance gains achieved by our proposed designs compared with non-IRS or IRS-OMA systems. Low complexity user ordering schemes and joint beamforming design with imperfect CSI are our future works.

APPENDIX A: PROOF OF THEOREM 1

Problem (P3.2) is a convex problem. Therefore, the optimal solution is characterized by the KKT conditions. Specifically, the Lagrangian function of Problem (P3.2) in terms of the active beamforming \mathbf{W}_k can be written as

$$\begin{aligned}
\mathcal{L} = & \sum_{j=1}^K \sum_{k \geq j}^K \lambda_{kj} \left(\text{Tr}(\mathbf{W}_k \mathbf{H}_j^H \mathbf{v} \mathbf{v}^H \mathbf{H}_j) - \frac{1}{S_{kj}} \right) \\
& + \sum_{k=1}^K \sum_{i < k}^K \beta_{ki}^j \left(\text{Tr}(\mathbf{W}_i \mathbf{H}_j^H \mathbf{v} \mathbf{v}^H \mathbf{H}_j) + \sigma^2 - I_{kj} \right) \\
& + \sum_{j=1}^K \sum_{i=1}^K \sum_{k \geq i}^K \mu_{ki}^j \left(\text{Tr}(\mathbf{W}_k \mathbf{H}_j^H \mathbf{v} \mathbf{v}^H \mathbf{H}_j) - \text{Tr}(\mathbf{W}_i \mathbf{H}_j^H \mathbf{v} \mathbf{v}^H \mathbf{H}_j) \right) \\
& + \alpha \left(P_T - \sum_{k=1}^K \text{Tr}(\mathbf{W}_k) \right) + \sum_{k=1}^K \text{Tr}(\mathbf{W}_k \mathbf{Y}_k) + \Upsilon,
\end{aligned} \tag{32}$$

where Υ denotes the collection of the optimization variables of the primal and dual problems and constant terms that are not relevant to the proof. λ_{kj} , β_{ki}^j , μ_{ki}^j and α denote the scalar Lagrange multipliers associated with constraints (16b), (16c), (16d) and (16e). \mathbf{Y}_k is the Lagrange multiplier matrix associated with the constraint (16f). The KKT conditions for the optimal \mathbf{W}_k^* are given by

$$\lambda_{kj}^*, \beta_{ki}^{j*}, \mu_{ki}^{j*}, \alpha^* \geq 0, \mathbf{Y}_k^* \succeq \mathbf{0}, \mathbf{Y}_k^* \mathbf{W}_k^* = \mathbf{0}, \nabla_{\mathbf{W}_k^*} \mathcal{L} = 0, \tag{33}$$

where λ_{kj}^* , β_{ki}^{j*} , μ_{ki}^{j*} , α^* and \mathbf{Y}_k^* denote the optimal Lagrange multipliers and $\nabla_{\mathbf{W}_k^*} \mathcal{L}$ represents the gradient of \mathcal{L} with respect to \mathbf{W}_k^* . Then, the condition $\nabla_{\mathbf{W}_k^*} \mathcal{L} = 0$ can be expressed as

$$\alpha^* \mathbf{I} = \mathbf{Y}_k^* + \mathbf{Z} \mathbf{v} \mathbf{v}^H \mathbf{Z}^H, \tag{34}$$

where \mathbf{Z} is given by

$$\mathbf{Z} = \sum_{j \leq k} \lambda_{kj}^* \mathbf{H}_j^H + \sum_{j=1}^K \sum_{i \leq k} \mu_{ki}^{j*} \mathbf{H}_j^H. \quad (35)$$

Multiplying both sides of (35) by \mathbf{W}_k^* and recalling that $\mathbf{Y}_k^* \mathbf{W}_k^* = \mathbf{0}$, we have $\alpha^* \mathbf{W}_k^* = \mathbf{Z} \mathbf{v} \mathbf{v}^H \mathbf{Z}^H \mathbf{W}_k^*$ and α^* is always positive. Applying basic rank inequalities for matrices, the following relations hold:

$$\text{rank}(\mathbf{W}_k^*) = \text{rank}(\alpha^* \mathbf{W}_k^*) = \text{rank}(\mathbf{Z} \mathbf{v} \mathbf{v}^H \mathbf{Z}^H \mathbf{W}_k^*) \leq \text{rank}(\mathbf{v} \mathbf{v}^H) = 1.$$

Therefore, $\text{rank}(\mathbf{W}_k^*) \leq 1$. The proof is completed.

APPENDIX B: SROCR APPROACH FRAMEWORK

We present a brief review of the SROCR approach in a general framework. Instead of ignoring the rank-one constraint, the main idea of the SROCR approach is that the rank-one constraint is relaxed gradually to find a feasible rank-one solution. Consider the following problem

$$(\text{P}) : \min_{\mathbf{X} \succeq 0} g_0(\mathbf{X}) \quad (36a)$$

$$\text{s.t. } g_k(\mathbf{X}) \preceq_k 0, k = 1, 2, \dots, K, \quad (36b)$$

$$\text{rank}(\mathbf{X}) = 1, \quad (36c)$$

where $g_k : \mathbb{C}^{N \times N} \rightarrow \mathbb{R}, k = 0, 1, 2, \dots, K$ are continuous and differentiable convex or affine functions of an $N \times N$ complex-valued positive semidefinite matrix variable $\mathbf{X} \succeq 0$, and \preceq_k can refer to " \leq " or " $=$ ". In order to handle the rank-one constraint (36c), we have the following problem

$$(\text{P}, \omega) : \min_{\mathbf{X} \succeq 0} g_0(\mathbf{X}) \quad (37a)$$

$$\text{s.t. } g_k(\mathbf{X}) \preceq_k 0, k = 1, 2, \dots, K, \quad (37b)$$

$$\lambda_{\max}(\mathbf{X}) \geq \omega^{(i)} \text{Tr}(\mathbf{X}), \quad (37c)$$

where $\lambda_{\max}(\mathbf{X})$ denotes the largest eigenvalue of \mathbf{X} . In particular, when $\omega^{(i)} \rightarrow 1$, solving the above problem can find a rank-one solution to Problem (P). When $\omega^{(i)} = 0$, the above problem is equivalent to the problem without the rank-one constraint. Motivated by this, we can increase

$\omega^{(i)}$ sequentially from 0 to 1 through iterations to make the constraint (37c) gradually approach the real rank-one constraint set. Specifically, $\lambda_{\max}(\mathbf{X})$ can be expressed as

$$\lambda_{\max}(\mathbf{X}) = u_{\max}(\mathbf{X}^{(i)})^H \mathbf{X} u_{\max}(\mathbf{X}^{(i)}), \quad (38)$$

where $u_{\max}(\mathbf{X}^{(i)})$ is the eigenvector corresponding to the largest eigenvalue of $\mathbf{X}^{(i)}$ and $\mathbf{X}^{(i)}$ is the obtained feasible solution from the previous iteration. The SROCR approach framework is summarized in **Algorithm 4**. Detailed discussion about the convergence can be found in [36], where it demonstrates that the sequence generated by the SROCR approach converges to a KKT stationary point of problem (P).

Algorithm 4 SROCR algorithm for Problem (P)

Initialize convergence thresholds $\epsilon_1, \epsilon_2, i = 0$.

Solve the relaxed problem (\mathbf{P}, ω) and obtain $\mathbf{X}^{(i)}$ when $\omega^{(i)} = 0$.

Define an initial step size $\delta^{(i)} \in (0, 1 - \lambda_{\max}(\mathbf{X}^{(i)})/\text{Tr}(\mathbf{X}^{(i)})]$.

- 1: **repeat**
 - 2: Given $\{\omega^{(i)}, \mathbf{X}^{(i)}\}$, solve the convex Problem (\mathbf{P}, ω) .
 - 3: **if** Problem (\mathbf{P}, ω) is solvable **then**
 - 4: Define the optimal solution as $\mathbf{X}^{(i+1)}$,
 - 5: $\delta^{(i+1)} = \delta^{(i)}$;
 - 6: **else** Problem (\mathbf{P}, ω) is solvable **then**
 - 7: $\delta^{(i+1)} = \delta^{(i)}/2$.
 - 8: **end**
 - 9: $\omega^{(i+1)} = \min \left(1, \frac{\lambda_{\max}(\mathbf{X}^{(i+1)})}{\text{Tr}(\mathbf{X}^{(i+1)})} + \delta^{(i+1)} \right)$.
 - 10: $i = i + 1$.
 - 11: **until** $\omega^{(i-1)} \geq \epsilon_1$ and $|g_0(\mathbf{X}^{(i)}) - g_0(\mathbf{X}^{(i-1)})| \leq \epsilon_2$.
-

REFERENCES

- [1] X. Mu, Y. Liu, L. Guo, C. Dong, J. Lin, and N. Al-Dhahir, "Sum rate maximization for intelligent reflecting surface aided multi-antenna NOMA communications," in *Proc. IEEE Int. Conf. Commun. (ICC)*, 2020.
- [2] M. D. Renzo, M. Debbah, D. T. Phan-Huy, A. Zappone, and M. Fink, "Smart radio environments empowered by reconfigurable AI meta-surfaces: an idea whose time has come," *EURASIP Journal on Wireless Communications and Networking*, vol. 2019, no. 1, 2019.
- [3] E. Basar, M. Di Renzo, J. De Rosny, M. Debbah, M. Alouini, and R. Zhang, "Wireless communications through reconfigurable intelligent surfaces," *IEEE Access*, vol. 7, pp. 116 753–116 773, 2019.
- [4] Y. Liu, Z. Qin, M. Elkashlan, Z. Ding, A. Nallanathan, and L. Hanzo, "Nonorthogonal multiple access for 5G and Beyond," *Proc. IEEE*, vol. 105, no. 12, pp. 2347–2381, Dec 2017.
- [5] Y. Cai, Z. Qin, F. Cui, G. Y. Li, and J. A. McCann, "Modulation and multiple access for 5G networks," *IEEE Commun. Surv. Tut.*, vol. 20, no. 1, pp. 629–646, Firstquarter 2018.

- [6] Z. Ding, Y. Liu, J. Choi, Q. Sun, M. Elkashlan, C. I, and H. V. Poor, "Application of non-orthogonal multiple access in LTE and 5G networks," *IEEE Commun. Mag.*, vol. 55, no. 2, pp. 185–191, February 2017.
- [7] Y. Liu, H. Xing, C. Pan, A. Nallanathan, M. Elkashlan, and L. Hanzo, "Multiple-antenna-assisted non-orthogonal multiple access," *IEEE Wireless Commun.*, vol. 25, no. 2, pp. 17–23, April 2018.
- [8] L. Lv, J. Chen, Q. Ni, Z. Ding, and H. Jiang, "Cognitive non-orthogonal multiple access with cooperative relaying: A new wireless frontier for 5G spectrum sharing," *IEEE Commun. Mag.*, vol. 56, no. 4, pp. 188–195, April 2018.
- [9] Z. Ding, P. Fan, and H. V. Poor, "Random beamforming in millimeter-wave NOMA networks," *IEEE Access*, vol. 5, pp. 7667–7681, 2017.
- [10] S. Timotheou and I. Krikidis, "Fairness for non-orthogonal multiple access in 5G systems," *IEEE Signal Process. Lett.*, vol. 22, no. 10, pp. 1647–1651, Oct 2015.
- [11] Z. Ding, P. Fan, and H. V. Poor, "Impact of user pairing on 5G nonorthogonal multiple-access downlink transmissions," *IEEE Trans. Veh. Technol.*, vol. 65, no. 8, pp. 6010–6023, Aug 2016.
- [12] J. Choi, "Power allocation for max-sum rate and max-min rate proportional fairness in NOMA," *IEEE Wireless Commun. Lett.*, vol. 20, no. 10, pp. 2055–2058, Oct 2016.
- [13] Z. Yang, Z. Ding, P. Fan, and N. Al-Dhahir, "A general power allocation scheme to guarantee quality of service in downlink and uplink NOMA systems," *IEEE Trans. Wireless Commun.*, vol. 15, no. 11, pp. 7244–7257, Nov 2016.
- [14] Y. Liu, Z. Ding, M. Elkashlan, and H. V. Poor, "Cooperative non-orthogonal multiple access with simultaneous wireless information and power transfer," *IEEE J. Sel. Areas Commun.*, vol. 34, no. 4, pp. 938–953, April 2016.
- [15] F. Fang, H. Zhang, J. Cheng, and V. C. M. Leung, "Energy-efficient resource allocation for downlink non-orthogonal multiple access network," *IEEE Trans. Commun.*, vol. 64, no. 9, pp. 3722–3732, Sep. 2016.
- [16] Y. Sun, D. W. K. Ng, Z. Ding, and R. Schober, "Optimal joint power and subcarrier allocation for full-duplex multicarrier non-orthogonal multiple access systems," *IEEE Trans. Commun.*, vol. 65, no. 3, pp. 1077–1091, March 2017.
- [17] M. F. Hanif, Z. Ding, T. Ratnarajah, and G. K. Karagiannidis, "A minorization-maximization method for optimizing sum rate in the downlink of non-orthogonal multiple access systems," *IEEE Trans. Signal Process.*, vol. 64, no. 1, pp. 76–88, Jan 2016.
- [18] Z. Ding, F. Adachi, and H. V. Poor, "The application of MIMO to non-orthogonal multiple access," *IEEE Trans. Wireless Commun.*, vol. 15, no. 1, pp. 537–552, Jan 2016.
- [19] Y. Liu, M. Elkashlan, Z. Ding, and G. K. Karagiannidis, "Fairness of user clustering in MIMO non-orthogonal multiple access systems," *IEEE Commun. Lett.*, vol. 20, no. 7, pp. 1465–1468, July 2016.
- [20] Z. Ding, R. Schober, and H. V. Poor, "A general MIMO framework for NOMA downlink and uplink transmission based on signal alignment," *IEEE Trans. Wireless Commun.*, vol. 15, no. 6, pp. 4438–4454, June 2016.
- [21] S. Ali, E. Hossain, and D. I. Kim, "Non-orthogonal multiple access (NOMA) for downlink multiuser MIMO systems: User clustering, beamforming, and power allocation," *IEEE Access*, vol. 5, pp. 565–577, 2017.
- [22] Y. Liu, Z. Qin, M. Elkashlan, Y. Gao, and L. Hanzo, "Enhancing the physical layer security of non-orthogonal multiple access in large-scale networks," *IEEE Trans. Wireless Commun.*, vol. 16, no. 3, pp. 1656–1672, March 2017.
- [23] F. Alavi, K. Cumanan, Z. Ding, and A. G. Burr, "Beamforming techniques for nonorthogonal multiple access in 5G cellular networks," *IEEE Trans. Veh. Technol.*, vol. 67, no. 10, pp. 9474–9487, Oct 2018.
- [24] Z. Ding, L. Dai, and H. V. Poor, "MIMO-NOMA design for small packet transmission in the Internet of Things," *IEEE Access*, vol. 4, pp. 1393–1405, 2016.
- [25] B. Wang, L. Dai, Z. Wang, N. Ge, and S. Zhou, "Spectrum and energy-efficient beamspace MIMO-NOMA for millimeter-wave communications using lens antenna array," *IEEE J. Sel. Areas Commun.*, vol. 35, no. 10, pp. 2370–2382, Oct 2017.

- [26] Q. Wu and R. Zhang, "Intelligent reflecting surface enhanced wireless network via joint active and passive beamforming," *IEEE Trans. Wireless Commun.*, pp. 1–1, 2019.
- [27] J. Chen, Y. Liang, Y. Pei, and H. Guo, "Intelligent reflecting surface: A programmable wireless environment for physical layer security," *IEEE Access*, vol. 7, pp. 82 599–82 612, June 2019.
- [28] M. Cui, G. Zhang, and R. Zhang, "Secure wireless communication via intelligent reflecting surface," *IEEE Wireless Commun. Lett.*, vol. 8, no. 5, pp. 1410–1414, Oct 2019.
- [29] Z. Ding and H. V. Poor, "A simple design of IRS-NOMA transmission," [Online]. Available:<https://arxiv.org/abs/1907.09918>.
- [30] G. Yang, X. Xu, and Y.-C. Liang, "Intelligent reflecting surface assisted non-orthogonal multiple access," [Online]. Available:<https://arxiv.org/abs/1907.03133>.
- [31] M. Fu, Y. Zhou, and Y. Shi, "Intelligent reflecting surface for downlink non-orthogonal multiple access networks," [Online]. Available:<https://arxiv.org/abs/1906.09434>.
- [32] Q. Wu and R. Zhang, "Beamforming optimization for intelligent reflecting surface with discrete phase shifts," in *Proc. IEEE Int. Conf. Acoust., Speech Signal Process. (ICASSP)*, May 2019, pp. 7830–7833.
- [33] H. Guo, Y.-C. Liang, J. Chen, and E. G. Larsson, "Weighted sum-rate optimization for intelligent reflecting surface enhanced wireless networks," [Online]. Available:<https://arxiv.org/abs/1909.06972>.
- [34] Y.-C. Liang, R. Long, Q. Zhang, J. Chen, H. V. Cheng, and H. Guo, "Large intelligent surface/antennas (LISA): Making reflective radios smart," [Online]. Available:<https://arxiv.org/abs/1906.06578>.
- [35] M. Grant and S. Boyd, "CVX: Matlab software for disciplined convex programming, version 2.1," [Online]. Available:<http://cvxr.com/cvx>, Mar 2014.
- [36] P. Cao, J. Thompson, and H. V. Poor, "A sequential constraint relaxation algorithm for rank-one constrained problems," in *2017 25th European Signal Processing Conference (EUSIPCO)*, Aug 2017, pp. 1060–1064.